

Steady-state Cluster Size Distribution in Stirred Suspensions


 Ruben D. Cohen

Department of Mechanical Engineering and Materials Science, Rice University, Houston, Texas 77251, USA


A combinatorial approach for predicting the steady-state agglomerate or drop-size distribution in batch suspensions undergoing intense stirring is proposed. The model accounts for the fact that both coagulation and break-up could occur simultaneously owing to agitation. Overall, considering its simplicity and the fact that it lacks any adjustable parameters, the results of the model compare favourably with experiment.

Owing to its widespread use in the chemical engineering field, the area of coagulation of fine particles or coalescence of liquid droplets has received considerable attention during the past few decades. At present there exists a vast amount of theoretical and experimental literature related to this area. The first and foremost is Smoluchowski's pioneering theory which provides a detailed, yet relatively simple explanation describing the kinetics of coagulation. This work was later expanded to include the effects of surface interactions and hydrodynamics on the rate of coagulation.

In conjunction with the numerous studies concerning coagulation and coalescence, there is an extensive literature on fragmentation [ref. (1) and (2) and references therein]. As it is basically the reverse of coagulation, fragmentation involves a time analysis of the break-up of a larger aggregate or drop into smaller fragments.

 In a system where only coagulation occurs, it is expected in theory that all particles eventually form one large cluster. On the other hand, fragmentation involves a continuous break-up of the initial aggregate until ultimately a monodisperse suspension, consisting only of the primary particles, is attained. In most practical situations, however, the two processes often act simultaneously to produce a suspension in which a large number of aggregates coexist at any instant of time, thereby leading to a specific transient size distribution. Interestingly, experiments show that after a relatively long time, the size distribution becomes independent of time. This occurs when the rate of coagulation equals that of break-up.

Coagulation and fragmentation can occur simultaneously owing to any kind of stirring or agitation. Agitation of the lowest intensity generally lies in the thermal regime and its corresponding energy is given by $k_B T$, where k_B is Boltzmann's constant and T is the absolute temperature. This yields an equilibrium size distribution that is primarily governed by the DLVO surface potential for colloidal particles.^{3,4} On the other hand, surface interaction loses its influence on equilibrium once stirring is intensified, *i.e.* by mechanical means. Here the relative velocities and the fluctuating forces which cause coagulation and fragmentation to occur simultaneously, are brought about by the mechanically induced turbulence of the surrounding fluid.

 Previous models for calculating steady-state size and weight distributions in batch suspensions undergoing both coagulation and break-up have typically been semi-empirical.^{5,6} The models, in many cases, go through very detailed numerical solutions of a population balance equation coupled with some type of fragmentation kinetics to yield the time-dependent size distributions. Carrying out these calculations to very long times ultimately yields the steady-state aggregate or drop-size distributions. These models generally tend to possess a number of empirical

parameters which have to be determined by experiments.

The primary objective of this work is to introduce an alternative approach for predicting the equilibrium or steady-state agglomerate or drop-size distribution in suspensions undergoing intense stirring. The main strength of this method, for which the derivation follows in the next section, is that it is relatively simple and requires no adjustable or empirical parameters.

Model Development

Consider a dilute monodisperse suspension containing N_0 primary colloidal particles each having a diameter equal to d_{\min} . These particles may either be solid or liquid droplets, and could very well be initially present in agglomerated or coalesced states. Intense mechanical stirring of the system causes certain agglomerates to break up and others to coagulate (or coalesce) simultaneously. Consequently, after a relatively long period of time, the system achieves equilibrium where a certain steady-state or time-independent agglomerate size distribution persists throughout the suspension. Experiments have shown that this final distribution is independent of the initial state, *i.e.* whether or not the primary particles were agglomerated before onset of mixing.⁷ Moreover, since the intense agitation would overshadow all energetics such as the DLVO interactions, then the final result would be an equilibrium condition independent of the energy state and determinable primarily by the combinatoric arguments described below.

The approach considered here is based on the assumption that after a sufficiently long period of time, all possible arrangements or groupings among the primary particles in the closed system can be achieved owing to isotropic stirring; in other words, the size distribution at steady state fluctuates equally between all possible states or groups. Fig. 1, for example, illustrates how four primary particles ($N_0 = 4$) can be arranged in groups belonging to five different categories (A-E). It should be emphasized that different possible configurations, *i.e.* cluster shapes, are assumed not to play an important role here.

Category A, which represents one arrangement, is a suspension that consists of four uncoagulated primary particles. Another possible grouping is category B in which the suspension contains two dimers. Since the particles are 'numbered', we find that the system can acquire this arrangement in three distinguishable ways. Category C is another probable grouping which contains a triplet and a primary particle. This can be achieved in four different ways. Category D, containing two separate primary particles and one dimer, can be achieved in six distinguishable ways. Finally, category E, which represents a suspension in which all particles have coagulated to form one cluster, is achievable in only one way. By the above reasoning, therefore, we note that since the

grouping		(N_1, N_2, N_3, N_4)	Ω
A	(1) (2) (3) (4)	(4, 0, 0, 0)	1
B	(1,2) (3,4)	(0, 2, 0, 0)	3
	(1,3) (2,4)		
	(1,4) (2,3)		
C	(3,1,2) (4) (1,3,4) (2)	(1, 0, 1, 0)	4
	(4,1,2) (3) (4,2,3) (1)		
D	(1) (2) (3) (4) (2) (3) (1) (4)	(2, 1, 0, 0)	6
	(1) (3) (2) (4) (2) (4) (1) (3)		
	(1) (4) (2) (3) (3) (4) (2) (1)		
E	(1,2,3,4)	(0, 0, 0, 1)	1

Fig. 1. Possible distinguishable groupings of four numbered primary particles.

occurrence of each distinguishable grouping in the categories mentioned is equally probable (neglecting energy and configurational effects), the steady state in a well mixed closed system containing four primary particles is capable of fluctuating between a total of 15 possible arrangements.

A more general, yet practical approach to this problem would be to introduce the degeneracy, $\Omega(N_1, N_2, N_3, \dots, N_{i_{\max}})$, as being the number of the distinguishable arrangements belonging to a certain grouping or category that the numbered primary particles can form. Here N_1 is the number of unattached or separate primary particles, N_2 is the number of dimers, N_3 is the number of agglomerates or drops containing three primary particles, and so on, all of them coexisting at any given instance of time in the suspension. Applying this to the case considered in fig. 1, the degeneracies for the groupings in categories A-E are, therefore, 1, 3, 4, 6 and 1, respectively.

Although derivation of the general form for the degeneracy (for any N_0) as applied to this situation is straightforward, it is nonetheless quite involved and lengthy, and therefore will not be presented here. Using combinatorics, however, we can show that

$$\Omega(N_1, N_2, N_3, \dots, N_{i_{\max}}) = \frac{N_0!}{\prod_{i=1}^{i_{\max}} N_i (i!)^{N_i}} \quad (1)$$

where i is the agglomerate size (in terms of number of primary particles) and i_{\max} is the size of the largest agglomerates that exist in the suspension. Although a more detailed discussion concerning the magnitude of i_{\max} appears later, we begin the analysis by assuming that

$$N_0 \gg i_{\max} \gg 1. \quad (2)$$

Eqn (1) is, of course, constrained by the number conservation, given by

$$N_0 = \sum_{i=1}^{i_{\max}} iN_i. \quad (3)$$

We must, in addition, note that although all of the groupings included in eqn (1) are indeed attainable, the probability of occurrence of a number of them, as determined by their degeneracies, would be less than others. In fig. 1, for example,

observing the system over a long period of time suggests that the state comprising a distribution of N_0 uncoagulated primary particles (category A, $\Omega = 1$) occurs much less frequently than that containing two separate primary particles and one dimer (category D, $\Omega = 6$). Consequently, there should in general exist a *most probable* size distribution for any N_0 greater than 2.

Returning now to eqn (1) and the subsequent restriction imposed by eqn (3), the next appropriate step is to obtain the most probable distribution of interest. In reference to the statistical mechanics literature, this is generally accomplished by means of Lagrange multipliers which can be used to extremize eqn (1) while satisfying eqn (3). We therefore express this as

$$\frac{\partial \ln \Omega}{\partial N_i} + \lambda \frac{\partial}{\partial N_i} \sum_{i=1}^{i_{\max}} iN_i = 0 \quad (4)$$

where λ is the yet unknown Lagrange multiplier. Moreover, from eqn (1)

$$\ln \Omega = \ln N_0! - \sum_{i=1}^{i_{\max}} (N_i \ln i! + \ln N_i!) \quad (5)$$

and after assuming that large numbers of any agglomerate or drop size are present, *i.e.*

$$N_i \gg 1 \quad (6)$$

then the Stirling approximation for $\ln N_i!$ can be implemented.⁸ Substituting the approximation into eqn (5), taking the derivative with respect to N_i , and inserting the final result into eqn (4), we obtain the most probable size distribution. Denoting this as \mathcal{N}_i , the result is

$$\mathcal{N}_i = \frac{\exp(\lambda i)}{i!} \equiv \frac{Z^i}{i!} \quad (7)$$

where for simplicity and convenience, the unknown $\exp \lambda$ has been replaced by the single parameter Z . The value of Z can be readily calculated upon substituting eqn (7) into eqn (3). This gives

$$N_0 = \sum_{i=1}^{i_{\max}} \frac{iZ^i}{i!} \quad (8)$$

which can also be expressed as

$$N_0 = Z \frac{\partial}{\partial Z} \sum_{i=1}^{i_{\max}} \frac{Z^i}{i!}. \quad (9)$$

Assuming (which will be shown later to be quite reasonable)

$$i_{\max} \gg Z \gg 1 \quad (10)$$

eqn (9) approaches

$$\begin{aligned} N_0 &\cong Z \frac{\partial}{\partial Z} (\exp Z - 1) \\ &= Z \exp Z \end{aligned} \quad (11)$$

by virtue of the fact that the series in eqn (9) approximately represents the Taylor expansion of $(\exp Z - 1)$ under the condition specified by eqn (10).

For N_0 large compared to 1, *i.e.* $N_0 > 10^5$, which is typical of suspensions, one can solve eqn (11) for Z explicitly in terms of N_0 . It follows that

$$\lim_{N_0 \gg 1} Z \cong \ln N_0 - \ln(\ln N_0 - \ln \ln N_0). \quad (12)$$

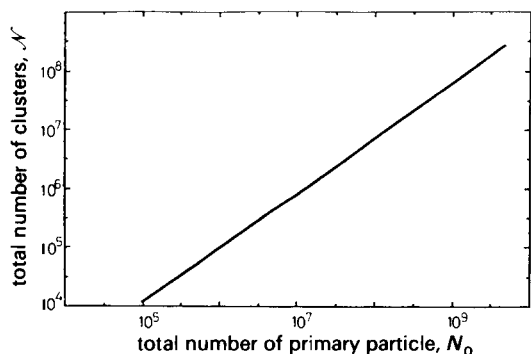


Fig. 2. Theoretical number of clusters, \mathcal{N} , vs. total number of primary particles, N_0 , in the suspension.

Two important parameters that are generally used in classifying agglomerates are the size and weight distribution functions, $P(i)$ and $W(i)$, respectively. For a given distribution N_i , these are defined as⁹

$$P(i) = \frac{N_i}{\sum_{i=1}^{i_{\max}} N_i} \quad (13)$$

and

$$W(i) = \frac{iN_i}{N_0} \quad (14)$$

Substitution of the most probable distribution, \mathcal{N}_i , from eqn (7) into eqn (13) and (14), therefore yields the most probable size and weight distribution functions, $\mathcal{P}(i)$ and $\mathcal{W}(i)$, respectively. Consequently,

$$\mathcal{P}(i) = \frac{\mathcal{N}_i}{\sum_{i=1}^{i_{\max}} \mathcal{N}_i}$$

which, by virtue of eqn (7), is just

$$\mathcal{P}(i) = \frac{Z^i/i!}{\sum_{i=1}^{i_{\max}} Z^i/i!} \quad (15)$$

We should emphasize that the denominator of eqn (15) is the most probable total number of aggregates, \mathcal{N} , at steady state. Therefore, based on a previous argument that $\exp Z \gg 1$, we get

$$\mathcal{N} \approx \exp Z.$$

This is illustrated in fig. 2 as \mathcal{N} vs. N_0 (total number of primary particles or droplets). It is rather interesting to observe that over the wide range indicated, \mathcal{N} generally falls below N_0 by a factor of about one order of magnitude.

It also follows that the most probable size distribution function becomes

$$\mathcal{P}(i) = \exp(-Z) \frac{Z^i}{i!} \quad (16)$$

which is the Poisson distribution. Fig. 3 displays the behaviour of $\mathcal{P}(i)$ vs. i as N_0 varies over several orders of magnitude.

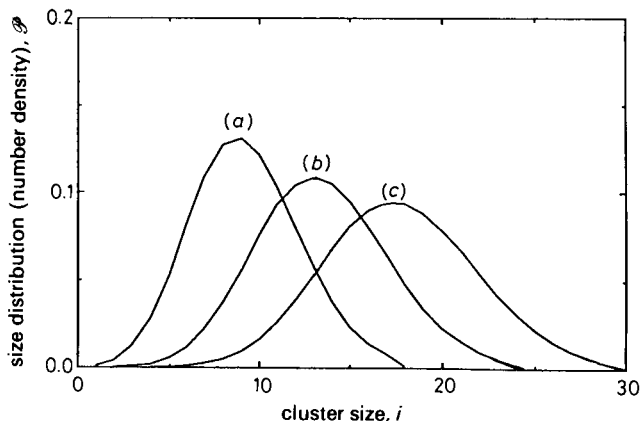


Fig. 3. Theoretical size distribution function, \mathcal{P} , vs. cluster size, i . N_0 : (a) 10^5 , (b) 10^7 , (c) 10^9 .

Moreover, the most probable weight distribution function, $\mathcal{W}(i)$, can be written as

$$\mathcal{W}(i) = \frac{i\mathcal{N}_i}{N_0} = \frac{iZ^i}{N_0 i!}$$

after inserting eqn (7) into (14). The above can be simplified further to yield

$$\mathcal{W}(i) = \exp(-Z) \frac{Z^{i-1}}{(i-1)!} = \mathcal{P}(i-1) \quad (17)$$

after substituting eqn (11) into the equation preceding (17). Interestingly, eqn (17) implies that the weight distribution curve is identical in shape to the size distribution but shifted to the right by one unit.

For coalescence, however, we may consider the smallest droplets (diameter d_{\min}) to be the primary particles. The result is that fig. 3 can be displayed in terms of the diameter ratio, where

$$\text{diameter ratio} \equiv d/d_{\min} = i^{1/3} \quad (18)$$

(d is the drop diameter) instead of the number of unit primary droplets, i , in a given drop of size i . This is illustrated in fig. 4. Altogether, we conclude the following:

1. All curves possess distinct maxima at some value of $i = i^*$. This can be calculated by extremizing eqn (16) with respect to i . Using the Stirling approximation for $\ln i!$, it can be shown that $\mathcal{P}(i)$ has a maximum at ca.

$$i = Z. \quad (19)$$

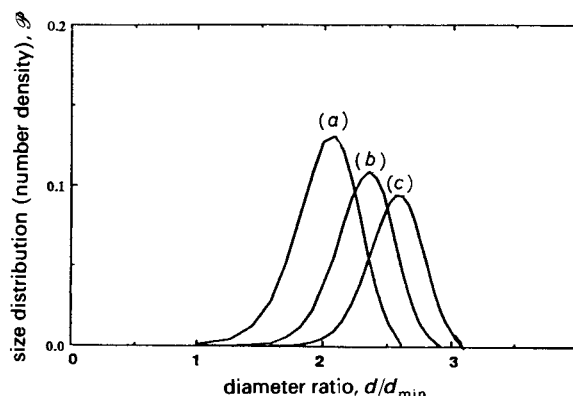


Fig. 4. Theoretical size distribution function, \mathcal{P} , vs. drop diameter ratio, d/d_{\min} . N_0 : (a) 10^5 , (b) 10^7 , (c) 10^9 .

Accordingly, in terms of the diameter ratio for coalescence, the maximum occurs at some diameter ratio, d/d_{\min} , given by

$$\frac{d}{d_{\min}} = \epsilon^{1/3} = Z^{1/3} \quad (20)$$

by virtue of eqn (18) and (19).

2. In reference to fig. 3 and 4, a decrease in N_0 shifts the \mathcal{P} curves towards smaller agglomerate or drop sizes, whereas an increase causes them to become wider and lower in height. Furthermore, whereas a plot of \mathcal{P} against i , as shown in fig. 3, is quite symmetric, \mathcal{P} vs. d/d_{\min} exhibits a certain degree of asymmetry leaning towards smaller diameter ratios.

3. Since \mathcal{N}_i is supposed to be an integer for any value of i , it would therefore be reasonable to define the maximum drop size, i_{\max} , by letting

$$\mathcal{N}_{i_{\max}} \approx 1. \quad (21)$$

Substituting this result into eqn (7) yields

$$\mathcal{N}_{i_{\max}} \approx 1 = \frac{Z^{i_{\max}}}{i_{\max}!} \quad (22)$$

from which, by virtue of the Stirling approximation for $\ln i_{\max}!$, we obtain

$$i_{\max} = eZ \approx 2.72Z \quad (23)$$

where Z is given by eqn (12). Note that since Z is of the order of 15 for very large N_0 , then the above provides reasonable justification for the assumption presented in eqn (10). In terms of the maximum drop diameter, d_{\max} , in the system, we therefore obtain the ratio

$$\frac{d_{\max}}{d_{\min}} = (\epsilon Z)^{1/3} \approx 1.40Z^{1/3}. \quad (24)$$

It is interesting to note that within the framework of the model, a maximum drop diameter ratio characterized only by the distribution controlling parameter, Z , can be calculated. In relation to works conducted on coalescing systems, the diameter of the primary drop, d_{\min} , is predominantly governed by surface tension, turbulence intensity, and other flow-related factors.¹⁰ As a result, eqn (24) implies that the maximum drop diameter, d_{\max} , would, in addition to the above-mentioned factors, be also affected by N_0 , although the influence is rather weak. Furthermore, eqn (24) suggests that all drops should lie within a relatively narrow range of diameter ratio given by

$$1 \leq \frac{d}{d_{\min}} < 1.40Z^{1/3} \quad (25)$$

4. Eliminating d_{\min} by combining eqn (20) and (24) gives the following

$$\frac{d}{d_{\max}} = \left(\frac{i}{i_{\max}}\right)^{1/3} = \exp(-1/3) \approx 0.72 \quad (26)$$

which implies that the ratio d/d_{\max} is virtually a constant, independent of all other variables.

5. In compliance with the parameters used here, the Sauter mean diameter, d_{32} , can be expressed as

$$\frac{d_{32}}{d_{\min}} = \frac{\sum_{i=1}^{i_{\max}} i^3 \mathcal{P}(i)}{\sum_{i=1}^{i_{\max}} i^2 \mathcal{P}(i)} \quad (27)$$

where $\mathcal{P}(i)$ is obtained from eqn (16). Eqn (27) was solved

Table 1. Comparison of the two characteristic diameters, d and d_{32}

N_0	d/d_{\min}	d_{32}/d_{\min}
10^5	2.104	2.127
10^6	2.251	2.271
10^7	2.383	2.400
10^8	2.503	2.517
10^9	2.614	2.626

numerically for certain values of N_0 and the results, along with d/d_{\min} obtained from eqn (20), are presented in table 1. In reference to the numbers given in table 1, we are therefore, able to conclude that d_{32} and d are very close to each other so that the Sauter mean diameter ratio can be approximately represented by

$$\frac{d_{32}}{d_{\min}} \approx \frac{d}{d_{\min}} = Z^{1/3} \quad (28)$$

in accordance with eqn (20).

6. In terms of the given parameters, the cumulative volume fraction, V , and the cumulative number fraction, n , can be written as

$$V(i) = \sum_{j=1}^i \mathcal{V}(j) \quad (29a)$$

$$n(i) = \sum_{j=1}^i \mathcal{P}(j) \quad (29b)$$

where j is just a dummy variable, and $\mathcal{P}(j)$ and $\mathcal{V}(j)$ come from eqn (16) and (17), respectively. Fig. 5 and 6, respectively, depict V as a function of the cluster size, i , and diameter ratio, d/d_{\min} . In this respect, it is useful to note that $V = 0.5$ corresponds approximately to d/d_{\min} , and therefore to

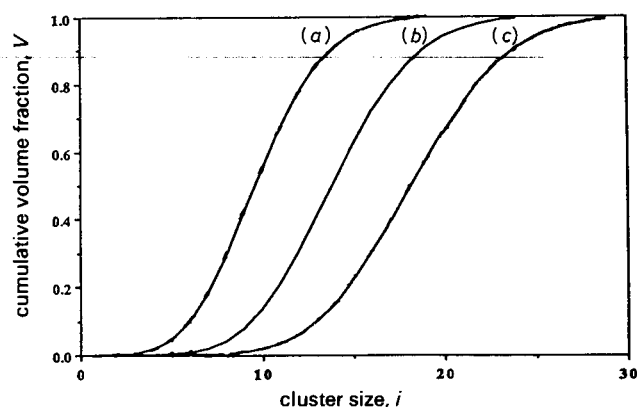


Fig. 5. Theoretical cumulative volume fraction, V , vs. cluster size, i . N_0 : (a) 10^5 , (b) 10^7 , (c) 10^9 .

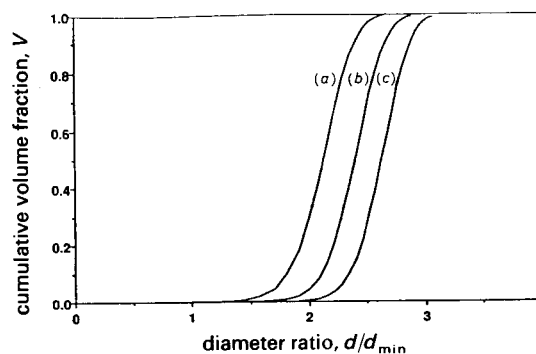


Fig. 6. Theoretical cumulative volume fraction, V , vs. drop diameter ratio, d/d_{\min} . N_0 : (a) 10^5 , (b) 10^7 , (c) 10^9 .

d_{32}/d_{\min} by virtue of eqn (28). Also, owing to eqn (17), $n(i)$ and $V(i)$ are expected to be similar in shape, but shifted slightly relative to each.

Comparison with Experimental Results and Conclusions

The experimental literature on cluster- or drop-size distributions in stirred suspensions is quite extensive. A large fraction of this presents empirical and semi-empirical equations relating the characteristic drop diameter in the vessel to the mixing conditions (given as Weber number or shear rate) and to the dispersed phase volume fraction or holdup [ref. (5), and references therein, (7), (11)–(17)]. Whereas the above studies are concerned mainly with steady-state conditions, there are others which deal with temporal developments of cluster size distributions in systems undergoing only break-up,^{2,6} coagulation [ref. (18) and references therein], or both at the same time [ref. (5) and some references therein].

We should note that some of the data mentioned above were collected from open or continuous flow operations [e.g. ref. (5) and (7)], whereas our model is based on batch systems. Comparison of the theory with data obtained from open systems, however, is justifiable provided that the residence timescales in these are much greater than the coalescence and break-up timescales. In Godfrey *et al.*⁵ and Ross *et al.*,⁷ we believe this criterion is satisfied to rightly enable us to compare their data with our batch model.

Overall, upon comparing the model with experimental data, we find that satisfactory agreement seems to exist between the two. For example, the experiments of Sprow¹⁶ and Godfrey *et al.*⁵ lead to the conclusion that d_{32}/d_{\max} is a constant, independent of other system variables. This observation agrees well with this work's prediction given by eqn (26). Note that $d_{32} \approx d$, as was found earlier. Table 2 provides the numerical constants of d_{32}/d_{\max} derived from the present work and the experimental results of Sprow¹⁶ and Godfrey *et al.*⁵

Interestingly, considering that Sprow's analysis assumes only break-up to occur (owing to the low dispersed phase volume fractions used), the results seem to be in reasonable agreement with our model. It is clear, however, that Sprow's distributions are wider than what our model predicts. In fact, we realize that, in general, systems undergoing only break-up yield distributions that are somewhat wider than the ones given here [i.e. see ref. (17)].

Upon plotting the theoretical ratio d_{32}/d_{\min} [using eqn (28)] in fig. 7, we find once again that our model compares favourably with the experiments of Ross *et al.*⁷ and Narsimhan *et al.*⁶ although the latter assumes that break-up dominates over coalescence. The present theory, however, overpredicts the ratio by a factor of ca. 1.25. We should mention that N_0 was estimated using the relationship

$$N_0 = \frac{6V\phi}{\pi d_{\min}^3} \quad (30)$$

where V is the total volume of the solution, and ϕ is the dispersed phase volume fraction. Furthermore, d_{\min} was taken to be the smallest diameter available from the steady-state dis-

Table 2. Comparison of the values for the ratio d_{32}/d_{\max} obtained from this work with related experiments

ref.	d_{32}/d_{\max}
this work	0.72
16	0.38
5	0.60

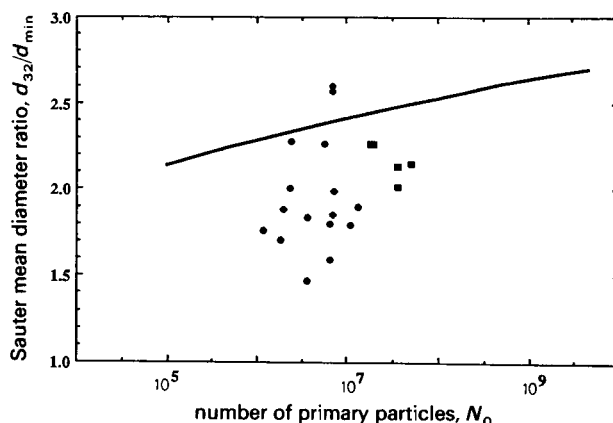


Fig. 7. Comparison of the theoretical and experimental Sauter mean diameter ratio, d_{32}/d_{\min} , vs. total number of primary particles, N_0 . Solid line is based on eqn (28) and the experimental points are taken from ref. (6) (■) and (7) (◆).

tribution data, and d_{32} was extracted from the volume-fraction data of Narsimhan *et al.*⁶ after considering that it should approximately coincide with a cumulative volume fraction of 0.50.

Finally, comparison of the theoretical cumulative number fraction, n , taken arbitrarily at $N_0 = 10^7$, with the experimental data of Godfrey *et al.*⁶ is shown in fig. 8. The indication here is that our model satisfactorily follows the trends of the data. Moreover, the order-of-magnitude agreement is quite good considering the absence of any adjustable parameters in the model.

Some other qualitative agreements of the model with experiments are that (i) the effects of the dispersed phase volume fraction on the drop volume distribution seem to be small,⁶ and (ii) an increase in N_0 widens the size distribution or \mathcal{P} curves and lowers their peaks (e.g. compare fig. 4 with the size distribution data of Ross *et al.*⁷).

Finally, upon focusing on the drawbacks of the proposed model, we note that many of the experimental works described above furnish distribution curves that are typically of the form shown in fig. 9 [i.e. see ref. (7) and (15)]. In contrast to our results depicted in fig. 4, we find that the model underestimates the maximum achievable drop sizes. Consequently, the experimental size distributions are somewhat wider than the ones predicted here. This is also evident from

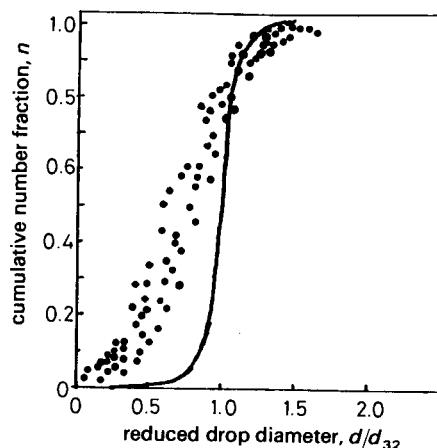


Fig. 8. Comparison of the theoretical and experimental cumulative number fraction, n , vs. reduced diameter ratio, d/d_{32} . Solid line is for an arbitrary $N_0 = 10^7$ and the experimental points are taken from ref. (5).

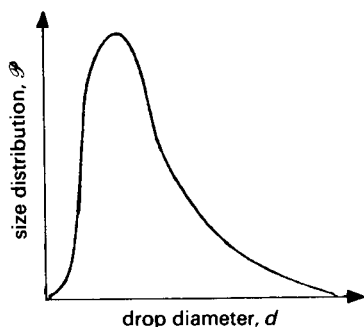


Fig. 9. Typical experimental curve showing size distribution, \mathcal{P} , vs. drop diameter, d .

table 2. At this time, we shall avoid any conclusive explanation for this discrepancy; however, we can only speculate that this may be due to our formulating the original problem in terms of discrete and distinguishable primary particles. Although this formulation appears to be sound for coagulation of solid particles, it may fail to apply to coalescence of liquid droplet simply because the break-up following the coalescence of two primary liquid droplets, identified as 1 and 2, may produce another pair of primary droplets which, although similar in size to the former ones, do not necessarily contain exactly the same material as the primary droplets, 1 and 2. Consideration of this factor would require a modification to the combinatoric relationship given by eqn (1).

In summary, we have proposed a simple model for obtaining the steady-state size distributions of agglomerates in stirred suspensions. Based on the assumption that surface interactions and energy-state effects are totally overwhelmed by the intense agitation, the model therefore relies only on combinatorics to predict results which happen to agree within reasonable bounds with the experimental data obtained from literature. Furthermore, the advantage of the present model over previous models is that it requires no adjustable or empirical parameters for data fitting.

Glossary

d	drop diameter
d	drop diameter at maximum value of \mathcal{P} [eqn (20)]
d_{\max}	maximum drop diameter [eqn (24)]
d_{\min}	diameter of primary droplets (minimum diameter)

i	cluster size
i	cluster size at maximum value of \mathcal{P} [eqn (19)]
i_{\max}	maximum cluster size in the system [eqn (23)]
k_B	Boltzmann constant
$n(i)$	cumulative number fraction [eqn (29b)]
\mathcal{N}	most probable total number of clusters in the system
\mathcal{N}_i	most probable number of clusters of size i in the system [eqn (7)]
N_i	number of clusters of size i in the system
N_0	total number of primary particles in the system
\mathcal{P}	most probable size distribution function or number density [eqn (16)]
P	size distribution function or number density [eqn (13)]
V	cumulative volume fraction [eqn (29a)]
W	weight distribution function [eqn (14)]
\mathcal{W}	most probable weight distribution function [eqn (17)]
Z	distribution characteristic [eqn (12)]
Ω	degeneracy [eqn (1)]

References

- 1 E. D. McGrady and R. M. Ziff, *AIChEJ.*, 1988, **34**, 2073.
- 2 D. L. Brown and C. E. Glatz, *Chem. Eng. Sci.*, 1987, **42**, 1831.
- 3 R. D. Cohen, *J. Stat. Phys.*, 1988, **51**, 559.
- 4 R. D. Cohen, *Powder Tech.*, 1989, **59**, 145.
- 5 J. C. Godfrey, F. I. N. Obi, and R. N. Reeve, *Chem. Eng. Prog.*, 1989, **85**, 61.
- 6 G. Narsimhan, D. Ramkrishna, and J. P. Gupta, *AIChEJ.*, 1980, **26**, 990.
- 7 S. L. Ross, F. H. Verhoff and R. L. Curl, *Ind. Eng. Chem. Fundam.*, 1978, **17**, 101.
- 8 C. M. Bender and S. A. Orszag, *Advanced Mathematical Methods for Scientists and Engineers* (McGraw-Hill, New York, 1978).
- 9 F. W. Billmeyer, *Textbook of Polymer Science* (Wiley, New York, 1984).
- 10 J. O. Hinze, *AIChEJ.*, 1955, **1**, 289.
- 11 Y. Mlynek and W. Resnick, *AIChEJ.*, 1972, **18**, 122.
- 12 L. B. Brakalov, *Chem. Eng. Sci.*, 1987, **42**, 2373.
- 13 A. N. Sembira, J. C. Merchuk and D. Wolf, *Chem. Eng. Sci.*, 1988, **43**, 373.
- 14 A. Prabhakar, G. Sriniketan and Y. B. G. Varma, *Can. J. Chem. Eng.*, 1988, **66**, 232.
- 15 G. Grossman, *Ind. Eng. Chem. Proc. Des. Dev.*, 1972, **11**, 537.
- 16 F. B. Sprow, *Chem. Eng. Sci.*, 1967, **22**, 435.
- 17 R. Shinnar, *J. Fluid Mech.*, 1961, **10**, 259.
- 18 T. K. Belval and J. D. Hellums, *Biophys. J.*, 1986, **50**, 479.

Paper 9/04472H; Received 17th October, 1989